SPE SPE-164259-MS

Fast Beam Migration using Plane Wave Destructor (PWD) Beam Forming

Alexander Mihai Popovici, Z-Terra Inc.
Nick Tanushev, Z-Terra Inc.
Ioan Sturzu, Z-Terra Inc.
Iulian Musat, Z-Terra Inc.
Constantine Tsingas, Saudi Aramco
Sergey Fomel, University of Texas at Austin

This paper was prepared for presentation at the SPE Middle East Oil and Gas Show and Exhibition held in Manama, Bahrain, 10–13 March 2013.

Abstract

Fast Beam Migration (FBM) is a super-efficient algorithm that is two orders of magnitude faster than the standard Kirchhoff depth migration, and at the same time images multi-pathing energy, a property that is typically associated with wave-equation migration algorithms. The faster imaging step allows for more iterations of velocity model building (50-100 iterations, instead of the current 7-10), which enable the processing team to enhance the seismic resolution and imaging of complex geologic structures. Improved velocity models in combination with FBM or wave-equation imaging can provide much greater resolution and accuracy than what can be accomplished today with standard imaging technology. This advanced imaging methodology will improve success rate and cost effectiveness for new deep-field discoveries, greatly reduce the turnaround time for large surveys, and also have applications in increasing recovery efficiency for the development of existing fields, or 4-D seismic monitoring of CO_2 injection and sequestration projects. This technology does not exist widely in the industry, is a fundamental advance, and is a necessary building block in any seismic processing system that uses wave-equation methods for imaging ultra-deep land and water, complex oil-and-gas reservoirs.

The idea of beam-based seismic imaging algorithms is not new. Hill (1990, 2001) developed a rigorous and powerful method of depth imaging following the classical Gaussian beam construction. This work has been extended in different ways by a number of researchers (da Costa et al., 1989; Nowack et al., 2003; Gray, 2005). The idea of fast beam migration was also explored by Gao et al. (2006) and found perhaps the most successful commercial implementation at Applied Geophysical Services (Masters and Sherwood, 2005; Sherwood et al., 2009). While building on top of the previous knowledge, we developed a principally new implementation of fast beam-based seismic imaging. Our approach is based on the following novel ideas:

1. An innovative method of beam forming by using automatic plane-wave destruction (Fomel, 2002). This method is the working engine in the Data Decomposition via Beam Forming part of the algorithm.

2. An innovative method of beam extrapolation and imaging. The method derives from ideas employed previously in wavepath and parsimonious migration (Sun and Schuster, 2003; Hua and McMechan, 2005) and oriented imaging (Fomel, 2003, 2007b).

In practice, the Fast Beam algorithm achieves its speed by using the dip information pre-computed from pre-stack data, in two steps: (1) a factor of 10-100 in speedup is achieved via beam forming, or beam decomposition of the input data, where the number of input data traces is reduced by a factor of 10-100; (2) a factor of 10-100 in speedup is obtained by spreading each input trace, or beam over a beam patch instead of a full aperture-volume, by using the approximate dip information. Thus a single sample is spread over a beam patch instead of a full

ellipsoid surface. The combined speed up gives a factor of 100-1,000 in decreased run-time. The performance of the FBM algorithm allows us to migrate a 3000 square kilometers dataset on 1000 CPUs in 20-30 minutes, enabling a truly interactive migration for velocity model building definition and refinement.

Short Review of Fast Beam Migration Components

Fast Beam Migration (FBM) is a fast method for producing seismic images. It takes the recorded seismic data and a velocity model and produces an image of the subsurface. A typical beam migration workflow contains the following steps:

1. *Beam Forming* – The seismic input data is analyzed for locally coherent events. The slope of these events is identified and the associated wavelet is recorded as a beam. Beams are multidimensional objects that contain the recording time, the position of the source and receiver, the incident wave angles at the source and the receiver, and the associated seismic wavelet. This step needs to be done only once since it is independent of velocity.
2. *Beam Propagation* – This stage finds the migration time for each beam using ray tracing. For each beam, two rays are traced – one from the source and one from the receiver using the slopes identified in the beam forming stage. The time at which the rays meet in the subsurface is the migration time. All of the beam parameters are propagated to this time. These parameters provide information on how to reconstruct the wave field in the subsurface to form the image.
3. *Image Forming* – The final stage is to form the seismic image using the propagated parameters from beam propagation. At this stage, we can output an offset gather seismic volume that can be used as the input for traditional tomography.

Theory of Beam Forming using PWD filters

Plane-wave destruction (PWD) filters, introduced by Claerbout (1992), characterize seismic data by a superposition of local plane waves. They are constructed as finite-difference stencils for the plane-wave differential equation. In many cases, a local plane-wave model is a very convenient representation of seismic data. We can define the basis of the plane-wave destruction filters as the local plane differential equation:

$$\frac{\partial P}{\partial x}+\sigma\frac{\partial P}{\partial t}=0 \qquad (1)$$

where P(t,x) is the wave field, and σ is the local slope, which may also depend on t and x. In the case of a constant slope, equation (1) has the simple general solution

$$P(t,x)=f(t-\sigma x), \qquad (2)$$

where f(t)is an arbitrary waveform. Equation (2) is the mathematical description of a plane wave. If we assume that the slope σ does not depend on t, we can transform equation (1) to the frequency domain, where it takes the form of the ordinary differential equation

$$\frac{\partial \bar{P}}{\partial x}+i\omega\sigma\bar{P}=0 \qquad (3)$$

And has the general solution:

$$\bar{P}(x)=\bar{P}(0)e^{i\omega\sigma x}, \qquad (4)$$

Where $\bar{P}$ is the Fourier transform of P. The complex exponential term in equation (4) simply represents a shift of a t-trace according to the slope σ and the trace separation x. In the frequency domain, the operator for transforming the trace at position (x-1) to the neighboring trace and at position x is a multiplication by $e^{i\omega\sigma}$. In other words, a plane wave can be perfectly predicted by a two-term prediction-error filter in the F-X domain:

$$a_0\,\bar{P}(x)+a_1\,\bar{P}(x-1)=0 \qquad (5)$$

where $a_0=1$ and $a_1=-e^{i\omega\sigma}$. The goal of predicting several plane waves can be accomplished by cascading several two-term filters. In fact, any F-X prediction-error filter represented in the Z-transform notation as

$$A(Z)=1+a_1Z+a_2Z^2+\cdots+a_nZ^n \qquad (6)$$

can be factored into a product of two-term filters:

$$A(Z) = (1 - Z_1 Z)(1 - Z_2 Z)\cdots(1 - Z_N Z) \quad (7)$$

where $Z_1, Z_2, \ldots Z_N$ are the zeroes of polynomial (6). Thus we can fit an infinite number of dips in our input data. In practice, the user sets the maximum number of dips at a single location, and typically that is a number less than 5. According to equation (5), the phase of each zero corresponds to the slope of a local plane wave multiplied by the frequency. Zeroes that are not on the unit circle carry an additional amplitude gain not included in equation (3).

In order to incorporate time-varying slopes, we need to return to the time domain and look for an appropriate analog of the phase-shift operator (4) and the plane-prediction filter (5). An important property of plane-wave propagation across different traces is that the total energy of the propagating wave stays invariant throughout the process: the energy of the wave at one trace is completely transmitted to the next trace. This property is assured in the frequency-domain solution (4) by the fact that the spectrum of the complex exponential $e^{i\omega\sigma}$ is equal to one. In the time domain, we can reach an equivalent effect by using an all-pass digital filter. In the Z-transform notation, convolution with an all-pass filter takes the form

$$\bar{P}_{x+1}(Z_t) = \bar{P}_x(Z_t)\frac{B(Z_t)}{B(\frac{1}{Z_t})} \quad (8)$$

where $P_x(Z_t)$ denotes the Z-transform of the corresponding trace, and the ratio $B(Z_t)/B(1/Z_t)$ is an all-pass digital filter approximating the time-shift operator $e^{i\omega\sigma}$. In finite-difference terms, equation (8) represents an implicit finite-difference scheme for solving equation (1) with the initial conditions at a constant *x*. The coefficients of filter $B(Z_t)$ can be determined, for example, by fitting the filter frequency response at low frequencies to the response of the phase-shift operator (Thiran, 1971).

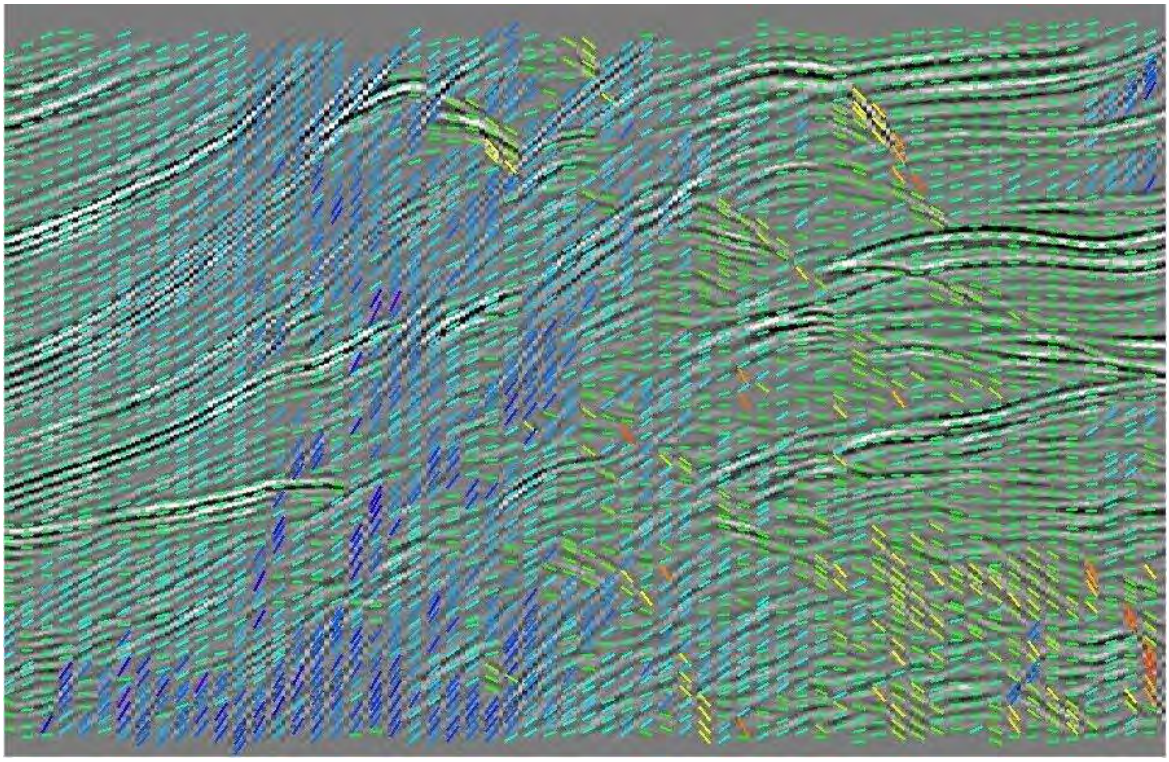

Figure 1: Prestack data decomposition in locally coherent events using PWD filters.

The first step of the FBM migration is the decomposition of the seismic data in seismic wavelets, 100-200 ms in time duration (Masters and Sherwood, 2005). The beam formation is performed directly in D(t,Sx,Sy,Gx,Gy) coordinates, where (Sx,Sy,Gx,Gy) are shot and receiver X,Y coordinates. Beams are formed on a uniform grid

with interals around 200-250 meters from traces that are collected in super-bins that are 200-500 meters wide in each of the spatial axes. Such a decomposition has additional regularization benefits, compensating for acquisition footprint and also control anti-aliasing even for very steep dips (Masters and Sherwood, 2005), thus FBM does not suffer from the aliasing effects typically encountered in the standard Kirchhoff migration.

Gaussian Beam Forming

We define a Gaussian beam (Fomel and Tanushev, 2009) as a seismic event characterized by a particular arrival time, location, amplitude, orientation, curvature, and extent. The extent of a beam is controlled by an amplitude taper, which can be understood as the imaginary part of a complex-valued event curvature. In the process of seismic imaging, the beam changes its position in time and space, as well as its amplitude, orientation, and complex curvature. Neglecting higher-order effects, a Gaussian beam representation is a powerful asymptotic approximation for describing different wave propagation phenomena (Popov, 1982; Babich and Popov, 1990; Bleistein and Gray, 2007; Kravtsov and Berczynski, 2007).

The first step of a beam-based processing strategy is decomposing the input data into Gaussian beams. The input data for many time-domain imaging steps are defined in *t*-*x* coordinates, where *t* is time and *x* is distance. The local traveltime curve at any given input location (t0, x0) can be expressed as the truncated series expansion:


. (9)

The local linear slope of the curve is determined by p_0, while *c* is a measure of the local parabolic curvature. A Gaussian beam centered at (t_0, x_0) can be constructed simply by allowing the curvature to be complex-valued ($c = c_r + ic_i$):


(10)

The curvature of the beam is still controlled by the real part of *c*, while the extent of the beam from the center is controlled by the imaginary part of *c*. Equation (10) also suggests there will be a real and an imaginary part of the traveltime itself (i.e., T = Tr +iTi). To confirm that this formula indeed constructs a Gaussian beam, b(*t, x*), one can look at the forward and inverse Fourier transforms for some input gather f(*T, x*),

$$b(t,x) = \frac{1}{2\pi}\int_{-\infty}^{\infty}\int_{-\infty}^{\infty} f(T,x)e^{-\omega T_i}e^{i\omega(T_r-t)}dTd\omega \tag{11}$$

to see the more familiar exponential form of the Gaussian function. One can now recognize the beam as the input event multiplied by a decaying Gaussian weight centered at (t_0, x_0), with a slope of p_0, and a curvature controlled by c_r.

Beam Forming on Irregular Geometry

Input data is typically not regularly sampled, so the dip estimation needs to be implemented for any input geometry. We used a high dimensional minimization based on the Nelder-Mead method to compute the dips. This allowed us to use any irregular input geometry, as sketched in Figure 2:

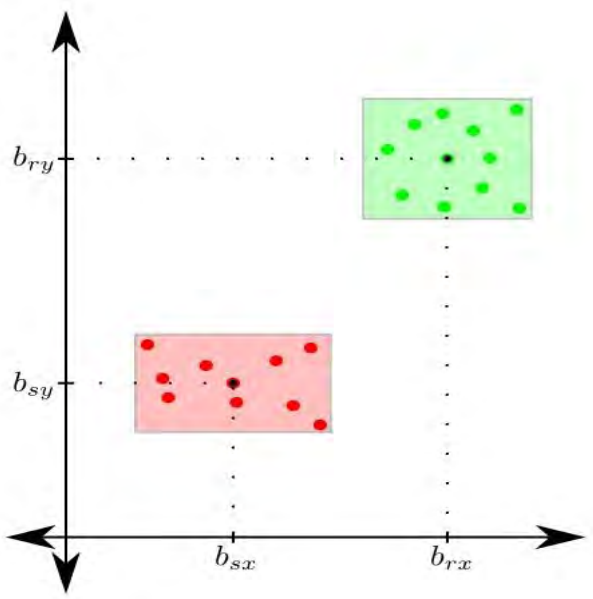

Figure 2: Using irregular geometry to estimate dips and seismic wavelet. The dots represent the seismic data coordinates at the receiver and the source.

Figure 3 shows a result with the latest version of beam forming and dip estimation code. The dips track the real seismic events very well, aliasing artifacts are minimal and the computation time well within the requirements for commercial applications.

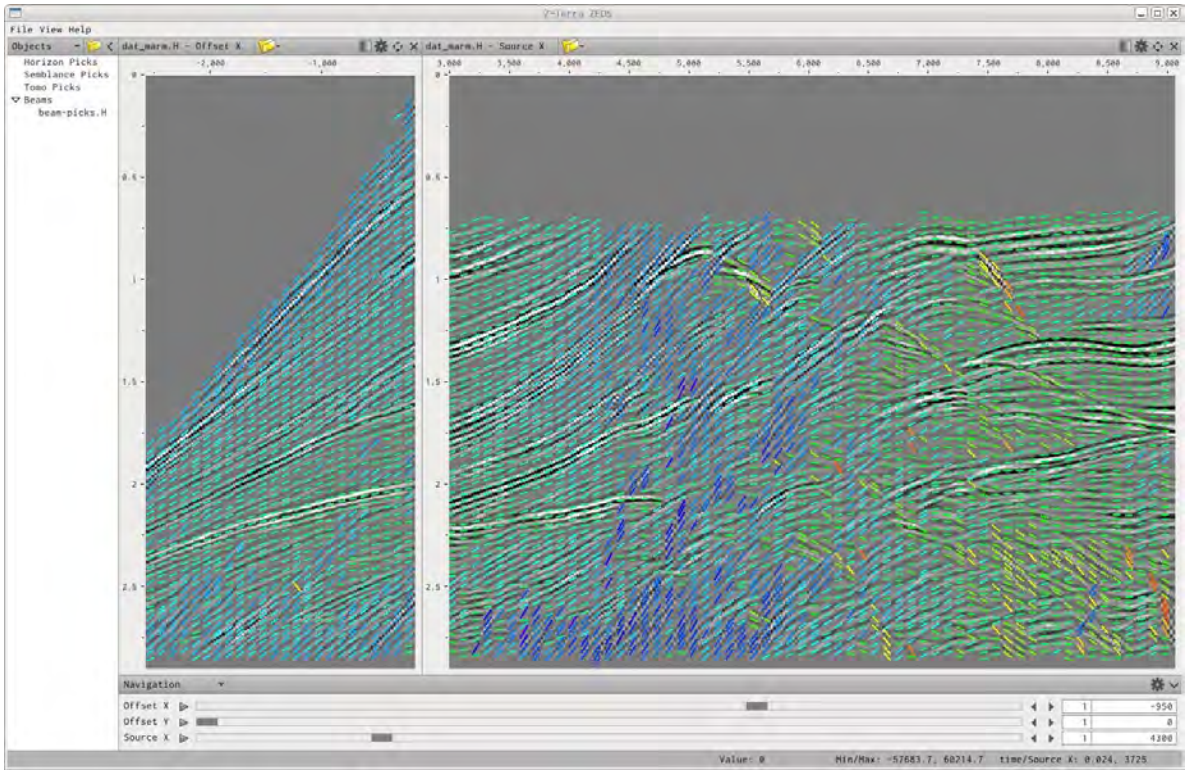

Figure 3: Beam forming for multi-dimensional data.

FBM Beam Propagation and Image Reconstruction

The beam wavelet with its auxiliary attributes is used to form a limited wavefront Kirchhoff migration for each pre-stack depth volume. Each beam wavelet is migrated separately, and by combining the effect from multiple beams to form the migration impulse response, we can observe local multi-pathing propagation. In addition, FBM does not suffer from the aperture limitations of the standard Kirchhoff implementation, allowing the imaging of very steep dips and overturning ray-paths while maintaining the complete aperture of the input data. This procedure allows for a higher signal to noise image compared to the standard Kirchhoff, where data from millions of traces may not have the necessary amplitude to cancel the migration swings in complex areas such as sub-salt. The true amplitude necessary for AVO friendly processing is also better preserved. Input wavelets can be excluded from the output image at this stage, for example by estimating the focusing quality factor, providing the means for reducing the coherent noise typically present in the deeper migrated areas. Finally, residual moveout can be applied to the migrated gathers for better final stacking, or used in successive tomography iterations for improving the velocity model.

In zero-offset migration, the source and receiver are at the same location and we only need to trace one ray to find the imaging location for the beam. In contrast with zero-offset migration, for pre-stack or 5-D beam migration, to find the imaging location for every beam, we need to trace two rays, one from the source and one from the receiver, and find the location at which the two rays meet. The rays must meet at the imaging location both in space and at the correct time, corresponding to the time at which the seismic event that the beam represents was recorded (See Figure 4 for a schematic view). To accomplish this, we trace both rays and find the meeting location by searching through the nearby possibilities. In real world examples the velocity model is not known precisely, also there are small errors in the estimated dips due to noise and accumulated errors from the ray tracing. All of these quantities contribute to the ray trajectories not being perfectly traced out in the model. Instead of the rays meeting in the subsurface they pass near each other and we have to use the closeness of the approach to estimate the exact meeting time. Since the beam attributes allow the travel time to be approximated in a neighborhood of the ray trajectory, we use this information to find the best meeting location. Note that this mismatch between the recording time and the migration time is exactly the type of information which is necessary for a tomographic update.

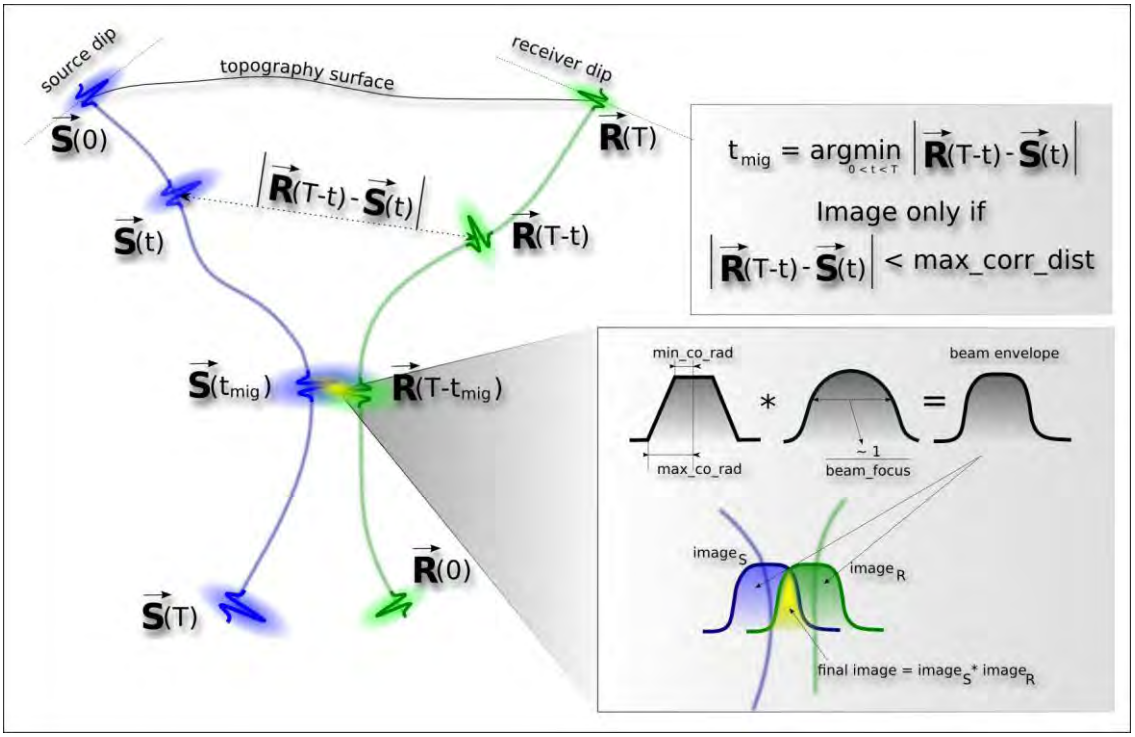

Figure 4: Source and receiver beam correlation and image forming.

Once the imaging location is found in the subsurface after the correlation step, the seismic wavelet that was identified in the beam forming stage has to be spread in a neighborhood of this location is a way that is consistent with the travel time approximation from the source and receiver beam attributes.

The beam attributes are used to approximate the travel time locally. For beams, the approximation is quadratic, so in addition to the standard ray tracing parameters (the position and direction of the ray) we need the Hessian matrix that describes the curvature of the travel time. A schematic version (in 1D) is shown in Figure 5.

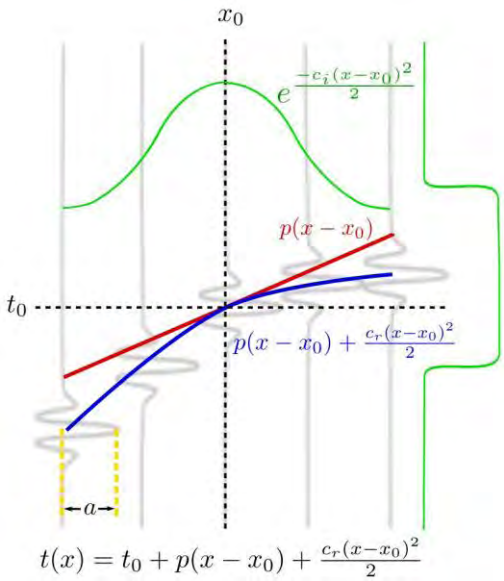

Figure 5: Quadratic travel time approximation in one dimension.

The beam attributes are traced using the following system of ordinary differential equations (ODEs)

$$\dot{\vec{x}}(t) = \frac{-c(\vec{x}(t))\vec{p}(t)}{|\,\vec{p}(t)\,|} \tag{12}$$

$$\dot{\vec{p}}(t) = |\,\vec{p}(t)\,|\,\nabla c(\vec{x}(t)) \tag{13}$$

$$\dot{M}(t) = -A(t) - M(t)B(t) - B^T(t)M(t) - M(t)C(t)M(t) \tag{14}$$

$$\dot{a}(t) = a(t)\left(\frac{-\vec{p}(t)\cdot\nabla c(\vec{x}(t))}{2\,|\,\vec{p}(t)\,|} - \frac{\vec{p}(t)\cdot M(t)\vec{p}(t)}{2\,|\,\vec{p}(t)\,|^3} + \frac{c(\vec{x}(t))Tr[M(t)]}{2\,|\,\vec{p}(t)\,|}\right) \tag{15}$$

The quantities used in these equations can be computed from the velocity $c(x)$:

$$A(t) = -\vec{p}(t)\nabla^2 c(\vec{x}(t)) \tag{16}$$

$$B(t) = \frac{-\vec{p}(t)}{|\,\vec{p}(t)\,|} \otimes \nabla c(\vec{x}(t)) \tag{17}$$

$$C(t) = \frac{-c(\vec{x}(t))}{|\,\vec{p}(t)\,|}\left(1 - \frac{\vec{p}(t)\otimes\vec{p}(t)}{|\,\vec{p}(t)\,|^2}\right) \tag{18}$$

Equations (12) and (13) are the standard ray tracing equation for the position, x, and the direction, p, of the ray.

Equations (14) and (15) represent the complex beam quadratic parameters.

One of the features of FBM that sets it apart from other types of migration such as reverse time migration or wave equation migration is that beam migration contains direct information about the connection between events in the seismic image and events in the input seismic data. This allows the user to visualize how different parts of the image are represented in the original input seismic data. In addition FBM can easily produce not only offset gathers, but also angle gathers which can be used for traditional tomography. Angle gathers are image volumes that are indexed by the angle in which the wave energy arrived at each image point. This information is already stored in beam, since we have the ray associated with each beam and the ray direction contains the arrival angle.

Data Examples

Figure 6 shows an FBM image of the Marmousi model and demonstrates the ability of the FBM algorithm to handle multiple arrivals, a feature difficult to implement in standard Kirchhoff migration, typically associated with wave-equation type algorithms. Figure 7 shows an impulse response using FBM in the Sigsbee velocity model and highlights the triplications in the impulse response operator that demonstrate the ability to image multi-pathing energy with FBM. Figures 8 and 9 shows a comparison between Kirchhoff and FBM depth migration of a real dataset**.**

Conclusions

We discuss the development details of Fast Beam Migration, an ultra-fast imaging algorithm based on the decomposition of the pre-stack data into locally coherent events, or beams, using PWD filters. FBM allows for very fast imaging iterations (order of minutes for imaging thousands of square kilometers), which combined with very fast migration velocity analysis tools, including wide-azimuth tomography provides much greater resolution and accuracy than what can be accomplished today with standard imaging technology. We show the application of the methodology with examples on synthetic and real data. FBM enables an order of magnitude more effective imaging of complex geologic structures.

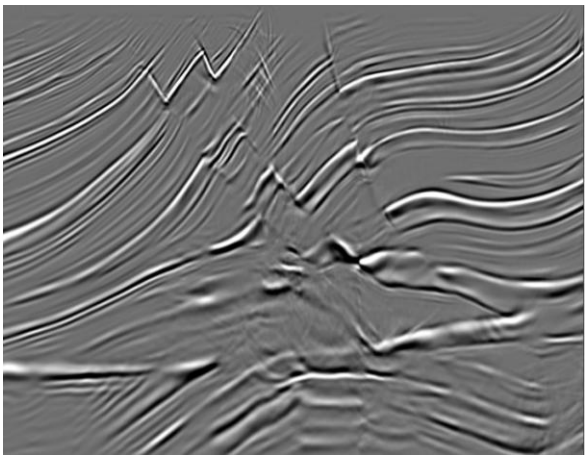

Figure 6: FBM Marmousi Image.

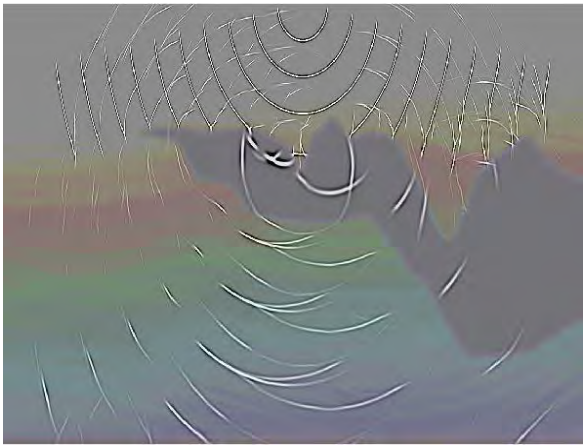

Figure 7: Sigsbee FBM impulse response.

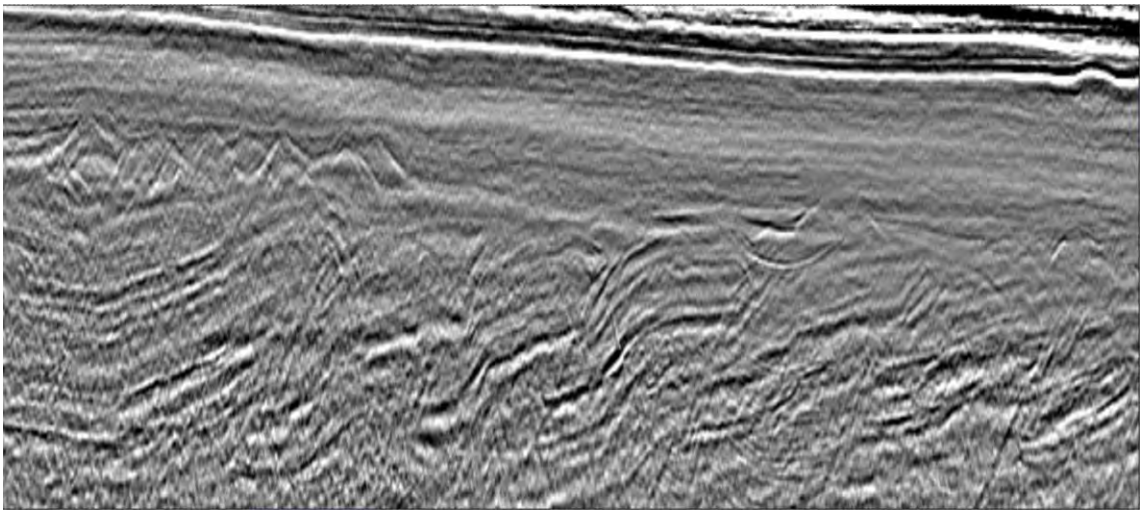

Figure 8: Kirchhoff depth migration. Data courtesy of Spectrum.

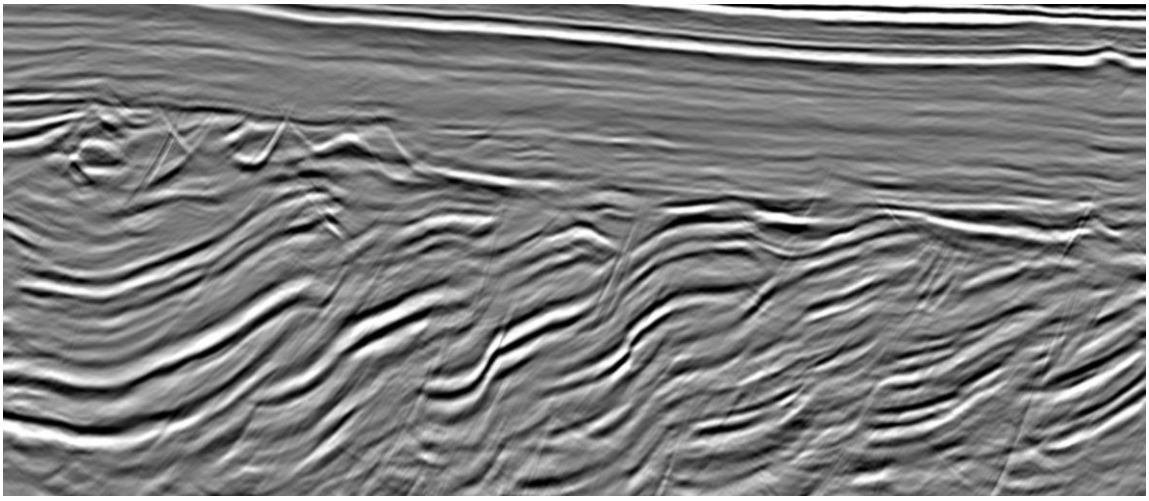

Figure 9: Fast Beam depth migration. Data courtesy of Spectrum.